Article

Structural and Thermodynamic Studies of the Interaction of Distamycin A with the Parallel Quadruplex Structure [d(TGGGGT)]

Luigi Martino, Ada Virno, Bruno Pagano, Antonella Virgilio, Simone Di Micco, Aldo Galeone, Concetta Giancola, Giuseppe Bifulco, Luciano Mayol, and Antonio Randazzo

J. Am. Chem. Soc., **2007**, 129 (51), 16048-16056 • DOI: 10.1021/ja075710k

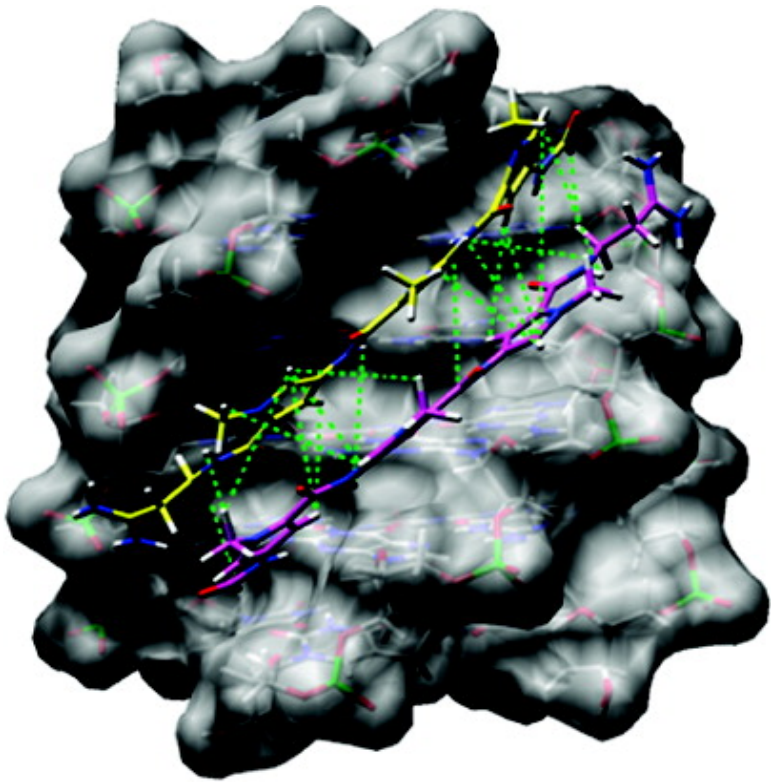

More About This Article

Additional resources and features associated with this article are available within the HTML version:

- Supporting Information
- Links to the 1 articles that cite this article, as of the time of this article download
- Access to high resolution figures
- Links to articles and content related to this article

J|A|C|S
ARTICLES
Published on Web 12/04/2007

Structural and Thermodynamic Studies of the Interaction of Distamycin A with the Parallel Quadruplex Structure $[d(TGGGGT)]_4$

Luigi Martino,[†] Ada Virno,[‡] Bruno Pagano,[§] Antonella Virgilio,[‡] Simone Di Micco,[§] Aldo Galeone,[‡] Concetta Giancola,[†] Giuseppe Bifulco,[§] Luciano Mayol,[‡] and Antonio Randazzo*[,‡]

Contribution from the Dipartimento di Chimica "P. Corradini", Università degli Studi di Napoli "Federico II", via Cintia, I-80126, Napoli, Italy, Dipartimento di Chimica delle Sostanze Naturali, Università degli Studi di Napoli "Federico II", via D. Montesano 49, I-80131 Napoli, Italy, and Dipartimento di Scienze Farmaceutiche, Università di Salerno, via Ponte Don Melillo, 84084, Fisciano (SA), Italy

Received July 31, 2007; E-mail: antonio.randazzo@unina.it

Abstract: The complex between distamycin A and the parallel DNA quadruplex $[d(TGGGGT)]_4$ has been studied by ^{1}H NMR spectroscopy and isothermal titration calorimetry (ITC). To unambiguously assert that distamycin A interacts with the grooves of the quadruplex $[d(TGGGGT)]_4$, we have analyzed the NMR titration profile of a modified quadruplex, namely $[d(TGG^{Me}GGT)]_4$, and we have applied the recently developed differential frequency-saturation transfer difference (DF-STD) method, for assessing the ligand−DNA binding mode. The three-dimensional structure of the 4:1 distamycin A/$[d(TGGGGT)]_4$ complex has been determined by an in-depth NMR study followed by dynamics and mechanics calculations. All results unequivocally indicate that distamycin molecules interact with $[d(TGGGGT)]_4$ in a 4:1 binding mode, with two antiparallel distamycin dimers that bind simultaneously two opposite grooves of the quadruplex. The affinity between distamycin A and $[d(TGGGGT)]_4$ enhances (∼10-fold) when the ratio of distamycin A to the quadruplex is increased. In this paper we report the first three-dimensional structure of a groove-binder molecule complexed to a DNA quadruplex structure.

Introduction

The ends of the chromosomes in all eukaryotic species have specialized noncoding DNA sequences that, together with associated proteins, are known as telomeres. Telomere protects the ends of the chromosome from damage and recombination and its shortening has been implicated in cellular senescence. Telomeric DNA consists of tandem repeats of simple short sequences, rich in guanine residues. In the presence of metal ions such as K^+ or Na^+, telomeric DNA can form structures of potential biological significance, the G-quadruplexes.[1] G-quadruplex structures comprise stacks of G-tetrads, which are the planar association of four guanines in a cyclic Hoogsteen hydrogen-bonding arrangement.[2] Telomerase, the enzyme which elongates the G-rich strand of telomeric DNA, is active in about 85% of tumors, leading the cancer cells to infinite lifetime. The inhibition of telomerase has become an attractive strategy for the anticancer therapy and, because telomerase requires a single-stranded telomeric primer, the formation of G-quadruplex complexes by telomeric DNA inhibits the telomerase activity. Furthermore, small molecules that stabilize G-quadruplex structures have been found to be effective telomerase inhibitors, and then the use of drugs to target G-quadruplexes is emerging as a promising way to interfere with telomere replication in the tumors cells and to act as anticancer agents.[3]

The truncated telomeric sequence from *Oxytricha*, d(TGGGGT), has been previously reported in literature to form a tetramer, with a parallel-stranded structure. This G-quadruplex has been determined by NMR and X-ray techniques; the strands associate generating a right-handed helix, containing four equivalent grooves and all bases in the *anti* glycosidic conformation.[4,5]

Distamycin A (Dist-A) is a small molecule with antibiotic properties which binds with high affinity to B-form DNA.[6,7] In particular, it has been demonstrated that two Dist-A molecules, side by side in an antiparallel orientation, are able to bind the expanded minor groove of an A and T rich regions of duplex DNA in a 2:1 drug/DNA stoichiometry.

[†] Dipartimento di Chimica "P. Corradini", Università degli Studi di Napoli "Federico II".
[‡] Dipartimento di Chimica delle Sostanze Naturali, Università degli Studi di Napoli "Federico II".
[§] Dipartimento di Scienze Farmaceutiche, Università di Salerno.

(1) Neidle, S.; Parkinson, G. N. *Curr. Opin. Struct. Biol.* **2003**, *13*, 275−283.
(2) Keniry, M. A. *Biopolymers* **2001**, *56*(3), 123−126.
(3) Kelland, L. R. *Eur. J. Cancer* **2005**, *41*, 971−979.
(4) Aboul-ela, F.; Murchie, A. I. H.; Norman, D. G.; Lilley, D. M. J. *J. Mol. Biol.* **1994**, *243*, 458−471.
(5) Laughlan, G.; Murchie, A. I.; Norman, D. G.; Moore, M. H.; Moody, P. C.; Lilley, D. M.; Luisi, B. *Science* **1994**, *265*, 520−524.
(6) Pelton, J. G.; Wemmer, D. E. *J. Am. Chem. Soc.* **1990**, *112*, 1393−1399.
(7) Chen, X.; Ramakrishnan, B.; Sundaralingam, M. *J. Mol. Biol.* **1997**, *267*, 1157−1170.

10.1021/ja075710k CCC: $37.00

Moreover, Dist-A has been shown to interact with four-stranded parallel DNA quadruplex containing oligonucleotides of different sequence.[8,9] Two opposite models have been proposed for the distamycin−quadruplex complex: the first, proposed by some of us, suggests that distamycin molecules bind as dimers in two opposite grooves of quadruplex [d(TGGGGT)]$_4$;[8] the second one suggests that two distamycin molecules stack on the terminal G-tetrad planes of the quadruplexes [d(TAGGGTTA)]$_4$, [d(TAGGGGTT)]$_4$, and [d(TAGGGGGT)]$_4$.[9] More recently, some distamycin analogues have been found interacting with a DNA quadruplex of sequence dGGG(TTAGGG)$_3$;[10] a mixed groove/G-quartet stacking binding mode was suggested for the interaction on the basis of molecular modeling. All these results suggest that, most probably, there is no general code that explains the drug−quadruplex binding and a sequence-dependent interaction could also be important. Since it is commonly believed that a deep understanding of factors which determine the complex formation and stabilization is important for the drug design, we tried to shed light on the binding mode of Dist-A to the quadruplex [d(TGGGGT)]$_4$, analyzing the NMR titration profile of a modified quadruplex, namely [d(TGG^{Me}GGT)]$_4$ (where dG^{Me} is 8-methyl-2′-deoxyguanosine) and applying the recently developed saturation transfer difference (STD) method.[11] Furthermore, we determined the three-dimensional structure of the Dist-A/[d(TGGGGT)]$_4$ complex by an in-depth NMR study followed by dynamic and mechanic calculations. We also report the energetics of the interaction by isothermal titration calorimetry (ITC).

All results unequivocally assess that distamycin molecules interact with [d(TGGGGT)]$_4$ in a 4:1 binding mode, with two distamycin dimers binding simultaneously two opposite grooves of the quadruplex.

Experimental Section

Oligonucleotide Synthesis. The oligonucleotides d(TGG^{Me}GGT) and d(TGGGGT) were synthesized on a Millipore Cyclone Plus DNA synthesizer using solid phase β-cyanoethyl phosphoramidite chemistry at 15 μmol scale. The synthesis of the suitably protected dG^{Me} phosphoramidite monomer was performed following the synthetic strategy proposed by Kohda et al.[12] with minor modifications. The oligomers were detached from the support and deprotected by treatment with concentrated aqueous ammonia at 55 °C for 12 h. The combined filtrates and washings were concentrated under reduced pressure, redissolved in H_2O, analyzed, and purified by high-performance liquid chromatography (HPLC) on a Nucleogel SAX column (Macherey-Nagel, 1000-8/46) using buffer A (20 mM KH_2PO_4/K_2HPO_4 aqueous solution (pH 7.0), containing 20% (v/v) CH_3CN) and buffer B (1 M KCl, 20 mM KH_2PO_4/K_2HPO_4 aqueous solution (pH 7.0), containing 20% (v/v) CH_3CN). A linear gradient from 0 to 100% B for 30 min and flow rate of 1 mL/min were used. The fractions of the oligomer were collected and successively desalted by Sep-pak cartridges (C-18). The isolated oligomers proved to be >98% pure NMR.

Nuclear Magnetic Resonance Experiments. NMR samples were prepared at a concentration of 2 mM, in 0.6 mL (H_2O/D_2O 9:1) buffer solution having 10 mM KH_2PO_4, 70 mM KCl, 0.2 mM EDTA, pH 7.0. For D_2O experiments, the H_2O was replaced with D_2O by drying down the sample, followed by lyophilization and redissolution in D_2O alone. NMR spectra were recorded with Varian ^{Unity}INOVA 700 MHz spectrometer. ^{1}H chemical shifts were referenced relative to external sodium 2,2-dimethyl-2-silapentane-5-sulfonate (DSS). 1D proton spectra of samples in H_2O were recorded using pulsed-field gradient DPFGSE[13,14] for H_2O suppression. Phase-sensitive NOESY spectra[15] were recorded with mixing times of 100 and 200 ms (T = 25 °C). Pulsed-field gradient DPFGSE sequence was used for NOESY experiments in H_2O. Pulsed-field gradient WATERGATE[16] sequence was used for ^{1}H-^{15}N HSQC[17] spectrum in H_2O. TOCSY spectra[18] with mixing times of 100 ms were recorded with D_2O solutions.

All experiments were recorded using STATES-TPPI[19] procedure for quadrature detection. In all 2D experiments, the time domain data consisted of 2048 complex points in $t2$ and 400−512 fids in $t1$ dimension. The relaxation delay was kept at 3 s for NOESY experiments used in the structure determination. A relaxation delay of 1.2 s was used for all other experiments. The NMR data were processed on a SGI Octane workstation using FELIX 98 software (Accelrys, San Diego, CA).

Structure Calculations. Cross-peak volume integrations were performed with the program FELIX 98, using the NOESY experiment collected at mixing time of 100 ms. The NOE volumes were then converted to distance restraints after they were calibrated using known fixed distances of H2′/H2″ of GA_5, TA_6, GB_3, GB_4, and GB_5. Then a NOE restraint file was generated with three distance classifications as follows: strong NOEs ($1.0 < r_{ij} < 3.5$ Å), medium NOEs ($3.0 < r_{ij} < 4.5$ Å) and weak NOEs ($4.0 < r_{ij} < 6.0$ Å). A total of 440 NOE-derived distance restraints were used.

Hydrogen bonds constraints were used ($1.7 < r_{ij} < 2.3$ Å). These constraints for H-bonds did not lead to an increase in residual constraints violation. A total of 96 backbone torsion angles were used in the calculations too. Particularly, the backbone torsion angles α, β, γ, δ, and ϵ were restrained in the range −150°/−30°, −230°/−110°, 20°/100°, 95°/175° and −230°/-110°, respectively, and glycosidic torsion angles χ were fixed in the *anti*-domain (−155°/-75°). Moreover, 64 planar constraints were used for G bases. The calculations have been performed using a distance dependent macroscopic dielectric constant of 4r, and an infinite cutoff for nonbonded interactions to partially compensate for the lack of the solvent has been used.[20] Thus the 3D structures which satisfy NOE and dihedral angle constraints were constructed by simulated annealing calculations.[21] An initial structure of the oligonucleotide was built using a completely random array of atoms. Using the steepest descent followed by quasi-Newton−Raphson method (VA09A), the conformational energy was minimized. Restrained simulations were carried out for 300 ps using the CVFF force field as implemented in Discover software (Accelrys, San Diego, CA). The simulation started at 500 K, and then the temperature was decreased stepwise until 100 K. The final step was again to energy-minimize to refine the obtained structures, using successively the steepest descent and the quasi-Newton−Raphson (VA09A) algorithms. Both dynamic and mechanic calculations were carried out by using 20 kcal mol^{-1} Å^{-2} flatwell distance restraints: 20 structures were generated. The rmsd

(8) Randazzo, A.; Galeone, A.; Mayol, L. *Chem. Commun.* **2001**, *11*, 1030−1031.
(9) Cocco, M. J.; Hanakahi, L. A.; Huber, M. D.; Maizels, N. *Nucleic Acids Res.* **2003**, *31*, 2944−2951.
(10) Moore, M. J. B.; Cuenca, F.; Searcey, M.; Neidle, S. *Org. Biomol. Chem.* **2006**, *4*, 3479−3488.
(11) Di Micco, S.; Bassarello, C.; Bifulco, G.; Riccio, R.; Gomez-Paloma, L. *Angew. Chem., Int. Ed.* **2006**, *45*, 224−228.
(12) Kohda, K.; Tsunomoto, H.; Minoura, Y.; Tanabe, K.; Shibutani, S. *Chem. Res. Toxicol.* **1996**, *9*, 1278−1284.
(13) Hwang, T. L.; Shaka, A. J. *J. Magn. Res.* **1995**, *A112*, 275−279.
(14) Dalvit, C. *J. Biomol. NMR* **1998**, *11*, 437−444.
(15) Jeener, J.; Meier, B.; Bachmann, H. P.; Ernst, R. R. *J. Chem. Phys.* **1979**, *71*, 4546−4553.
(16) Piotto, M.; Saudek, V.; Sklenar, V. J. *J. Biomol. NMR* **1992**, *2*, 661−665.
(17) Sklenar, V.; Piotto, M.; Leppik, R.; Saudek, V. *J. Magn. Reson.* **1993**, *102*, 241−245.
(18) Braunschweiler, L.; Ernst, R. R. *J. Magn. Reson.* **1983**, *53*, 521−528.
(19) Marion, D.; Ikura, M.; Tschudin, R.; Bax, A. *J. Magn. Reson.* **1989**, 85, 393−399.
(20) Weiner, S. J.; Kollman, P. A.; Case, D. A.; Singh, U. C.; Ghio, C.; Alagona, G.; Profeta, S.; Weimer, P. *J. Am. Chem. Soc.* **1984**, *106*, 765−784.
(21) Martino, L.; Virno, A.; Randazzo, A.; Virgilio, A.; Esposito, V.; Giancola, C.; Bucci, M.; Cirino, G.; Mayol, L. *Nucleic Acids Res.* **2006**, *34* (22), 6653−6662.

(root-mean-square deviation) value of 0.28 ± 0.069 Å for heavy atoms was calculated for the best ten structures. Illustrations of the structures were generated using the INSIGHT II program, version 2005 (Accelrys, San Diego, CA), Chimera,[22] Python,[23] APBS,[24] and MSMS.[25] All the calculations were performed on a PC running Linux WS 4.0.

The final set of coordinates has been deposited in the Protein Data Bank (accession code: 2JT7).

Isothermal Titration Calorimetry. The binding energetics was obtained with a CSC 4200 calorimeter from Calorimetry Science Corporation (CSC, Utah) at 25 °C. Calorimetric titrations were carried out by injecting 15 μL aliquots of a 300−900 μM ligand solution into a 30−50 μM quadruplex solution at 400 s intervals with stirring at 297 rpm at 25 °C for a total of 16 injections. Titration curves were corrected for heat of dilution determinated by injecting the ligand into the buffer.

The solutions of Dist-A (Sigma-Aldrich) and quadruplex DNA samples were prepared in the same buffer. Control experiments were done by injecting distamycin in buffer to obtain the heat effects for dilution of the drug. The calorimetric enthalpy for each injection was calculated after correction for the heat of Dist-A dilution. To obtain the thermodynamic properties of interaction, a nonlinear regression analysis was performed using two simple sets of independent binding-site model.[26]

STD Experiments. STD-NMR experiments were performed on a Bruker Avance DRX 600-MHz spectrometer equipped with cryoprobe, at 27 °C. NMR samples were prepared by dissolving the ligands and the $[d(TGGGGT)]_4$ oligomer in 200 μL (3 mm NMR tube) of a solution H_2O/D_2O (90:10) (20 μL, 99.996%, Sigma Aldrich) containing phosphate buffered saline (10 mM) at pH 7.1. A high ligand−quadruplex molar excess (50:1) was used for the best STD effects. In particular, the concentration of ligands was set at 4.5 mM. The concentration of the tetrastranded DNA olygomer was 90 μM.

Typically, 32 scans were recorded for the reference STD spectrum, whereas 64 scans were recorded for each DF−STD spectrum (saturation time = 4 s). The water ^{1}H signal was suppressed using a 3−9−19[17] pulse sequence. The STD effects of the individual protons were calculated for each compound relative to a reference spectrum with off-resonance saturation at $\delta = -16$ ppm.

The calculated binding mode indexes (BMIs) are

$$\mathrm{BMI} = \frac{\sum_i \left(\frac{\mathrm{SN}_{\mathrm{aromatic}}/\mathrm{SN}_{\mathrm{rif}}}{\mathrm{SN}_{\mathrm{aliphatic}}/\mathrm{SN}_{\mathrm{rif}}} \right)}{n_i} \quad (1)$$

$$\mathrm{BMI}' = \frac{\sum_i \left(\frac{\mathrm{SN}_{\mathrm{imino}}/\mathrm{SN}_{\mathrm{rif}}}{\mathrm{SN}_{\mathrm{aliphatic}}/\mathrm{SN}_{\mathrm{rif}}} \right)}{n_i} \quad (2)$$

$$\mathrm{BMI}'' = \frac{\sum_{\mathrm{i}} \left(\frac{\mathrm{SN}_{\mathrm{imino}}/\mathrm{SN}_{\mathrm{rif}}}{\mathrm{SN}_{\mathrm{aromatic}}/\mathrm{SN}_{\mathrm{rif}}} \right)}{n_i} \quad (3)$$

where $SN_{aliphatic}$, $SN_{aromatic}$, and SN_{imino} are the differences between the intensities (expressed as S/N ratio) of the signals of the drug when irradiated in the on-resonance STD spectrum (i.e., in the aliphatic, aromatic, and imino regions, respectively) and that of the signals in the off-resonance NMR spectrum. SN_{rif} is instead the intensity of the same signal in the off-resonance spectrum (see Experimental Section), and n_i is the number of the signals.

Results

Synthesis and NMR Titration of the Quadruplex $[d(TGG^{Me}GGT)]_4$. To clarify the binding mode of Dist-A with the quadruplex $[d(TGGGGT)]_4$, we have designed and synthesized a new oligonucleotide, namely $d(TGG^{Me}GGT)$, where dG^{Me} is 8-methyl-2′-deoxyguanosine, potentially capable of forming a quadruplex structure and possessing a bulky group (methyl) into the grooves. A NMR sample of $d(TGG^{Me}GGT)$ was prepared at a concentration of 2 mM, in 0.6 mL of (H_2O/D_2O 9:1) buffer solution having 10 mM KH_2PO_4, 70 mM KCl, 0.2 mM EDTA, pH 7.0. The sample was heated for 5−10 min at 80 °C and slowly cooled down to room temperature, then ^{1}H NMR spectra of it were recorded by using a DPFGSE pulse sequence for H_2O suppression.[13,14] The ^{1}H NMR spectrum (700 MHz, T = 25 °C) shows the presence of four well-defined singlets in the region 11−12 ppm, attributable to imino protons involved in Hoogsteen hydrogen bonds of G quartets (Figure 1, molar ratio = 0).

Moreover, the presence of five signals, belonging to three guanine H8 and two thymine H6 protons in the aromatic region, and of a methyl resonance at δ_H 2.24 ppm (attributable to dG^{Me}) indicates that a single well-defined quadruplex species is present in solution, consisting of four G-tetrads and possessing a fourfold symmetry with all strands parallel to each other. The entire pattern of NOEs observed in the NOESY experiment (700 MHz, T = 25 °C, mixing time 100 ms) (see Supporting Information) indicates that $d(TGG^{Me}GGT)$ forms a tetramolecular parallel quadruplex possessing a right-handed B-form helix structure and that the backbone conformations resemble closely that of the $[d(TGGGGT)]_4$. Noteworthy, the direct comparison of the intensities of the NOESY cross-peaks between H8 (Me-8 in the case of dG^{Me}) proton bases and sugar H1′, and between H8/Me-8 proton bases and sugar H2′/H2″ resonances indicates that, exactly as in $[d(TGGGGT)]_4$,[4,5] all Gs residues (including dG^{Me}) adopt an *anti* glycosidic conformation.

Thus, the quadruplex $[d(TGG^{Me}GGT)]_4$ has been titrated with Dist-A and the results are reported in Figure 1. The initial addition of 1 mol equiv of Dist-A to the quadruplex caused the downfield shift of the signal at δ_H of 7.30 belonging to the H6 proton of T6. The progressive increase of Dist-A concentration up to 4 mol equiv caused only a drift of DNA signals and drug resonances to gradually grow in intensity (between 6 and 7 ppm). A further addition of drug did not lead to significant changes.

Differential Frequency-STD Method. The binding mode of Dist-A with the quadruplex $[d(TGGGGT)]_4$ has also been deepened by means of the differential frequency-STD (DF-STD)[11] method. This method consists in an acquisition of a set of experiments at different saturation frequencies, and it can provide useful information on binding mode of DNA interacting molecules, discriminating among base-pair intercalators, minor groove binders, and external backbone binders.

In its original version, where duplex-DNA is investigated, the DF-STD method is based on the acquisition of two parallel sets of STD experiments performed under the same experimental conditions, irradiating on aromatic protons of purine/pyrimidine

(22) Pettersen, E. F.; Goddard, T. D.; Huang, C. C.; Couch, G. S.; Greenblatt, D. M.; Meng, E. C.; Ferrin, T. E. *J. Comput. Chem.* **2004**, *25* (13), 1605−1612.
(23) Michel, F. S. *J. Mol. Graphics Mod.* **1999**, *17*, 57−61.
(24) Baker, N. A.; Sept. D.; Joseph, S.; Holst. M. J.; McCammon, J. A. *Proc. Natl. Acad. Sci. U.S.A.* **2001**, *98*, 10037−10041.
(25) Sanner, M. F.; Spehner, J. C.; Olson, A. J. *Biopolymers* **1996**, *38* (3), 305−320.
(26) Freire, E.; Mayorga, O. L.; Straume, M. *Anal. Chem.* **1990**, *62*, 950−959.

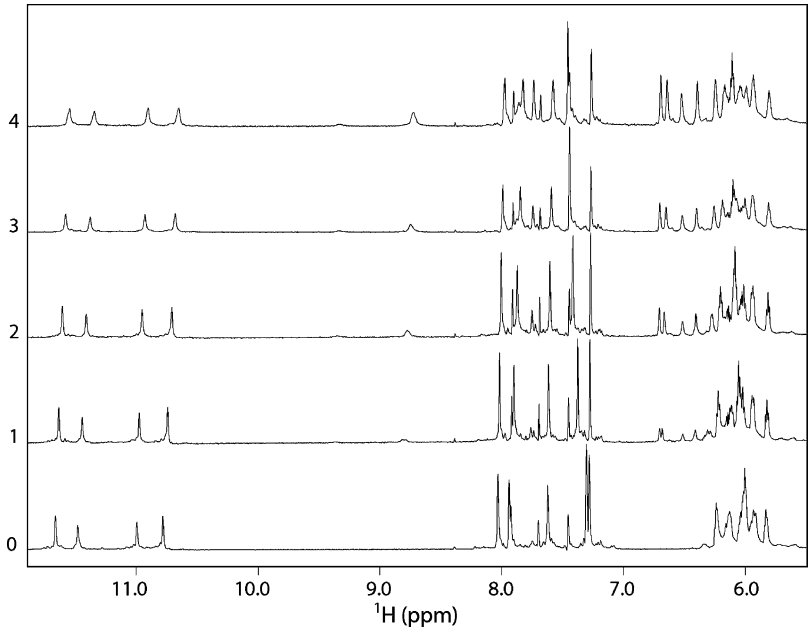

Figure 1. NMR titration of [d(TGG^{Me}GGT)]$_4$ with Dist-A. The drug/quadruplex molar ratios are shown along the side of the spectra.

Table 1. BMI Values for Ligands **1** and **2** Calculated by Using Equations 1−3 (See Experimental Section)

ligand	BMI	BMI′	BMI″
ethidium bromide	1.3	0.8	0.7
distamycin A	0.8	0.2	0.4

bases and on deoxyribose/backbone resonances[11] (both spectral regions where no ligand resonances were present).[27,28] In the present work we have used a third saturation frequency that is in the range of the imino proton frequencies, since such protons, pointing inside the quadruplex core, may be very diagnostic for probing this structural portion of the DNA quadruplex.

For our investigation, we have first employed a known DNA ligand, the ethidium bromide, a base-pairs intercalator which also interacts with the phosphate backbone thanks to its two charged amino group,[29,30] and then we used the Dist-A.

The aim to use this intercalator is to correctly interpret the experimental outcomes at different saturation frequency in the presence of a DNA quadruplex as biological target, considering the established binding mode to DNA. For Dist-A, the saturation frequencies are 11.0, 9.0, and 5.1 ppm, whereas for ethidium bromide they are 11.0, 9.5, and 2.4 ppm. The results of the irradiations for Dist-A and ethidium bromide are reported in the Supporting Information. We have calculated three binding mode indexes (BMIs)[11] for both molecules (see eqs 1−3 in the Experimental Section) and the results are reported in Table 1.

NMR Study. As already reported,[8] the NMR titration profile of [d(TGGGGT)]$_4$ with Dist-A is peculiar. An increase of Dist-A concentration up to 2 mol equiv caused drug resonances to gradually grow in intensity and a progressive drift of DNA signals. Nearly at 2:1 ligand/quadruplex stoichiometry, a further addition of drug caused a complication of the spectrum due to the appearance of a separate set of proton resonances. The intensities of these new resonances rose by increasing the amount of drug with the concomitant falling off of the original signals which completely disappeared at a ratio of 4:1 drug/quadruplex. The final NMR spectrum showed that the binding of the ligand to the quadruplex caused the loss of the original fourfold symmetry of the free quadruplex. Particularly, 8 imino proton, 4 methyl, and 12 aromatic proton resonances were discernible in the 1D proton spectra of the complex, counting for two pairs of not magnetically equivalent strands (named A and B).

An almost complete assignment (see Supporting Information) of the nonexchangeable/exchangeable protons of the complex has been accomplished by means of a combination of the analysis of 2D NOESY (700 MHz, 25 °C), TOCSY spectra (700 MHz, T = 25 °C), and ^{1}H-^{15}N HSQC experiments (700 MHz for ^{1}H, 70 MHz for ^{15}N, T = 25 °C). In particular, as for DNA, ^{1}H resonances within each deoxyribose were identified by 2D TOCSY experiment, while the analysis of NOEs among base protons and H1′, H2′, and H2″ protons allowed us to assign all base protons. It is interesting to note that the direct comparison of the intensities of the NOESY cross-peaks (700 MHz, T = 25 °C, mixing time 100 ms; see Supporting Information) between the H8 proton bases and sugar H1′ resonances and among H8 proton bases and sugar H2′/H2″ resonances indicates that all Gs residues of the complexed DNA adopt an *anti* glycosidic conformation. Then, all bases have classical H8/H2′-H2″ sequential connectivities to neighboring 5′ (see Supporting Information), indicating that the four strands are involved in the formation of a helical structure. Moreover, the entire pattern of NOEs observed indicates that the backbone conformations closely resemble that of the uncomplexed [d(TGGGGT)]$_4$ possessing a right-handed B-form helix structure.

Guanine imino protons and Dist-A amide and amidinium protons were first identified by means of an ^{1}H-^{15}N HSQC experiment. Thus, eight exchangeable protons correlate with ^{15}N in the region between 139.2 and 144.6 ppm, indicating that they

(27) Mayer, M.; Meyer, B. *Angew. Chem., Int. Ed.*, **1999**, *38*, 1784−1788.
(28) Mayer, M.; Meyer, B. *J. Am. Chem. Soc.* **2001**, *123*, 6108−6117.
(29) Luedtke, N. W.; Liu, Q.; Tor, Y. *Chem. Eur. J.* **2005**, *11*, 495−508.
(30) Guo, Q.; Lu, M.; Marky, L. A.; Kallenbach, N. R. *Biochemistry*, **1992**, *31*, 2451−2455.

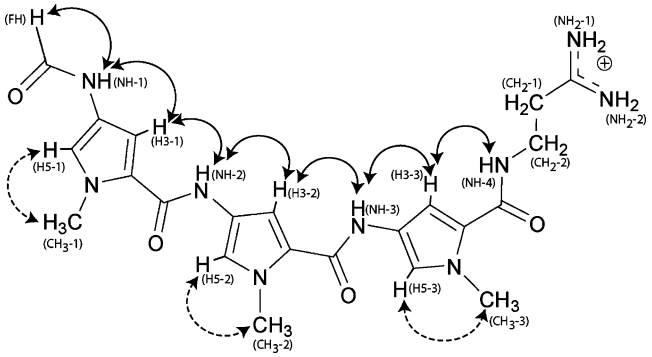

Figure 2. NOE connectivities observed within the Dist-A molecule. Regular and dashed lines represent connectivities on the concave and convex side of the molecule, respectively. Nomenclature used for Dist-A is reported in brackets (in gray).

are attributable to imino protons of G residues.[31] Furthermore, four other exchangeable protons correlate with ^{15}N in the region between 110.6 and 130.8 ppm, indicating that they are attributable to amide protons of Dist-A, and two exchangeable protons correlate with ^{15}N in the region between 80.4 and 80.7 ppm indicating that they are attributable to amidinium protons of Dist-A (see Supporting Information).

Each exchangeable proton signal was then assigned to the pertinent hydrogen by an in-depth analysis of the NOESY spectra. In particular, as far as DNA is concerned, NOEs among H1 protons at δ_H 10.62 and 10.68, and two methyl protons at δ_H 1.52 and 1.94 (belonging to T1_A and T1_B residues, respectively) led us to identify the imino protons belonging to the tetrad that is in proximity of the 5′ edge of the quadruplex. At the same way, NOEs among H1 protons at δ_H 10.80 and 10.62 ppm and the methyl groups at δ_H 1.74 and 1.75 ppm of the thymines T6_A and T6_B, respectively, led us to identify the imino protons belonging to the tetrad that is in proximity of the 3′ edge. The other four H1 resonances of the remaining two central tetrads were identified by analyzing the NOE connections with adjacent tetrads.

The resonances of Dist-A were assigned by first identifying the resonances belonging to the hydrogen on the convex side of the molecule (Figure 2).

Particularly, the H5 pyrrole protons (δ_H 6.66, 6.72, and 6.51 ppm for H5-1, H5-2, and H5-3, respectively) have been assigned taking into account that they both exhibit scalar and dipolar coupling with methyls that are linked to the same pyrrole ring (δ_H 3.39, 3.55, and 3.40 ppm for CH_3-1, CH_3-2, CH_3-3, respectively). As for the protons on the concave side of Dist-A, they have been assigned following the sequential NOE starting from the formyl proton at δ_H 7.70 ppm to the adjacent NH-1 (δ_H 9.80 ppm) and then sequentially to all other H3/NH hydrogens (Figure 2).

The NOESY spectrum of the complex contains many intermolecular drug/drug and drug/DNA NOEs, in addition to intramolecular ones. Particularly, as for drug/drug contacts, 9 head-to-tail NOEs for each Dist-A molecule (counting for 18 NOE contacts for each dimer) were clearly discernible in the NOESY spectra (Table 2). In addition, 22 NOEs were observed between Dist-A and $[d(TGGGGT)]_4$, predominantly involving aromatic protons of strand A and H1′ protons of strand B (Figure 3 and Table 3).

Table 2. Intermolecular Head-to-Tail Drug−Drug NOE Contacts

FH	CH_2
H3−1	H3−3
H5−2	CH_3−3, H5−3
H5−3	CH_3−2, H3−1, CH_3−1
NH−3	NH−2
NH−4	CH_3−1

Structure Calculations. To obtain the three-dimensional structure of the 4:1 complex at the atomic level, an estimation of proton−proton distances has been retrieved from cross-peak intensities in 2D NOESY experiments (700 MHz, $T = 25$ °C). Pseudoatoms were introduced where needed. A total of 440 distances were used for the calculations and, as suggested by the presence of eight guanine imino protons in the 1D ^{1}H NMR spectrum, 32 supplementary distance restraints (HN1−O6, HN2−N7) for 32 hydrogen bonds corresponding to the four G-quartets were also incorporated during the computations (Table 4).

In agreement with NMR data, the backbone torsion angles α, β, γ, δ, and ϵ were restrained in the range −150°/−30°, −230°/−110°, 20°/100°, 95°/175° and −230°/−110°, respectively.[32] Further, glycosidic torsion angles χ were fixed in the anti domain (−155°/−75°). Therefore, 3D structures which satisfy NOEs were constructed by simulated annealing (SA) calculations. An initial structure of the 4:1 complex was constructed possessing a random conformation and minimized. Restrained simulations were carried out for 300 ps using the CVFF (consistent valence force field).

The restrained SA (simulated annealing) calculations started at 500 K, and thereafter, the temperature was decreased stepwise down to 100 K. The aim was to energy-minimize and refine the structures. A total of 20 structures was generated. An average rmsd value of 0.28 ± 0.069 Å for the heavy atoms was obtained from the superimposition of the best 10 structures (Figure 4).

Isothermal Titration Calorimetry Measurements. ITC was used to provide direct information about the interaction enthalpy ($\Delta H°$), binding constant (K_b), and stoichiometry (n).[33] In addition, to fully characterize the thermodynamics of the binding reactions, we determined the change in free energy ($\Delta G°$) and entropy ($T\Delta S°$).

Figure 5 shows the ITC results for the titration of $[d(TGGGGT)]_4$ with Dist-A. The interaction heats were corrected for the heats of dilution associated with the addition of Dist-A into buffer solution. Fitting of the corrected data allows $\Delta H°$, K_b, and n to be determined (Table 5).

ITC measurements show that the affinity of Dist-A toward $[d(TGGGGT)]_4$ follows the same behavior observed by NMR; there are two distinct binding events, with 2:1 and 4:1 drug/quadruplex stoichiometry, respectively. Examination of the thermodynamic data reveals that Dist-A/$[d(TGGGGT)]_4$ interactions are exothermic. K_b values of 4×10^5 M^{-1} and 4×10^6 M^{-1} have been found for 2:1 and 4:1 complexes, respectively.

Discussion

To unambiguously assert that Dist-A interacts with the grooves of the quadruplex $[d(TGGGGT)]_4$, we have designed and synthesized a new modified oligonucleotide, namely d(TG-G^{Me}GGT). Particularly, we have taken advantage of the finding

(31) Fernández, C.; Szyperski, T.; Ono, A.; Iwai, H.; Tate, S.; Kainosho, M.; Wüthrich, K. *J. Biomol. NMR* **1998**, *12*, 25−37.
(32) Wüthrich, K. *NMR of Protein and Nucleic Acids;* Wiley: New York, 1986.
(33) Haq, I.; Ladbury, J. *J. Mol. Recognit.* **2000**, *13*, 188−197.

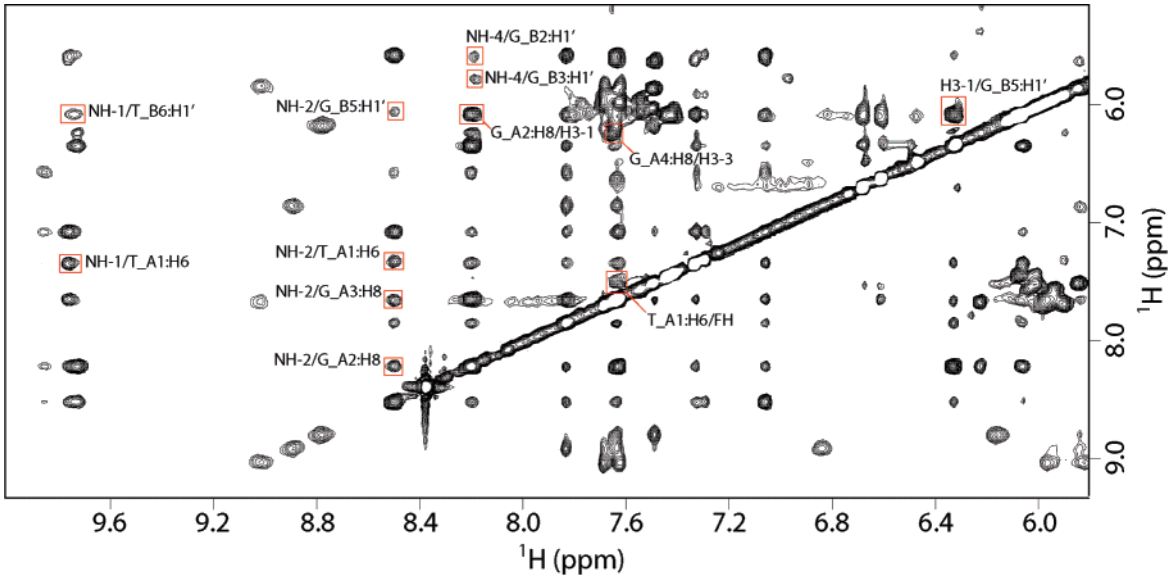

Figure 3. Expanded region of the NOESY (700 MHz, 25 °C, mt=100 ms) spectrum of the 4:1 complex Dist-A/[d(TGGGGT)]$_4$, displaying some of the intermolecular drug−DNA NOE contacts (boxed in red).

Table 3. Intermolecular Drug−DNA NOE Contacts

drug proton	DNA proton
FH	G5_B:H1, T1_A:H6
NH−1	G2_B:H1, T1_A:CH$_3$, T6_B:H1′, T1_A:H6
NH−2	G5_B:H1′, T1_A:H5″, G2_A:H8, T1_A:H6, G3_A:H8
NH−3	G3_A:H8
NH−4	G2_B:H1′, G3_B:H1′
H3−1	G5_B:H1′, T1_A:H2″, G2_A:H8
H3−3	G4_A:H8, G3_B:H1
H5−1	T1_A:H2′
CH$_3$−2	G2_A:H2′, G5_B:H5″

Table 4. Experimental Constraints and Structure Statistics of the Best 10 Structures

experimental constraints	
total NOEs	440
NOEs from nonexchangeable protons	352
NOEs from exchangeable protons	88
hydrogen bonds constraints	32
dihedral angle constraints	96
planarity constraints for G bases	64
CVFF energy (kcal mol^{-1}) of the minimized structures	
total	1187.44 ± 3.78
nonbond	−148.27 ± 3.48
restraint	226.06 ± 2.14
NOEs violations	
number >0.2 Å	0.4 ± 0.1
maximum (Å)	0.196 ± 0.028
sum (Å)	3.026 ± 0.232
average violation (Å)	0.007
r.m.s. deviations from the mean structure (Å)	
all heavy atoms	0.28 ± 0.069

of a recent study of some of us[34] concerning the aptitude of 8-methyl-2′-deoxyguanosine (dG^{Me}) containing oligonucleotides to form quadruplex structures. According to the NMR data, the oligonucleotide d(TGG^{Me}GGT) is actually able to fold into a quadruplex, and its structure is almost superimposable to that of [d(TGGGGT)]$_4$. Thus, each 8-methyl group of the four dG^{Me} of the quadruplex [d(TGG^{Me}GGT)]$_4$ faces right in to the very central region of the grooves, pointing outward the quadruplex. As a result, if Dist-A interacts with the groove of the quadruplex, the presence of these bulky groups in the very central region of the four grooves should prevent (or at least should limit) the insertion of Dist-A molecules, and consequently, the formation of a stable complex.

(34) Virgilio, A.; Esposito, V.; Randazzo, A.; Mayol, L.; Galeone, A. *Nucleic Acids Res.* **2005**, *33*(19), 6188−6195.

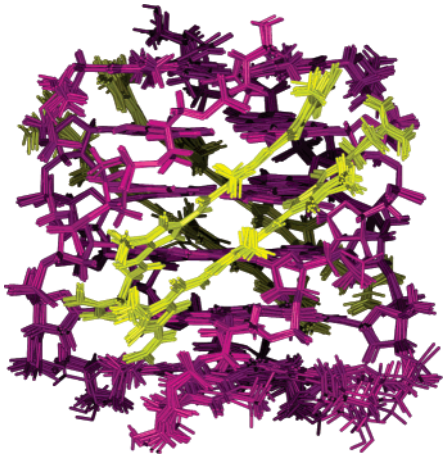

Figure 4. Side view of the superimposition of the 10 best structures of the 4:1 complex Dist-A/[d(TGGGGT)]$_4$. Dist-A is reported in yellow, and DNA is colored in magenta.

In the case of [d(TGGGGT)]$_4$, Dist-A displayed a high affinity toward the quadruplex as suggested by the appearance of a new set of signals during the NMR titration. Furthermore, Dist-A caused the loss of the original 4-fold symmetry of the free quadruplex. On the other hand, during the entire titration process of quadruplex [d(TGG^{Me}GGT)]$_4$, the four strands were magnetically equivalent, and only a general change of the chemical shift resonances could be observed (Figure 1). This behavior could be explained assuming that really the presence of the methyl groups in the central region of the grooves does affect the binding of Dist-A to the quadruplex, and hence that Dist-A interacts with the grooves of the quadruplex.

The interaction of Dist-A with the grooves of the quadruplex [d(TGGGGT)]$_4$ was further inferred by the analysis of the DF-STD data by using the binding mode indexes (BMIs)[11] (see

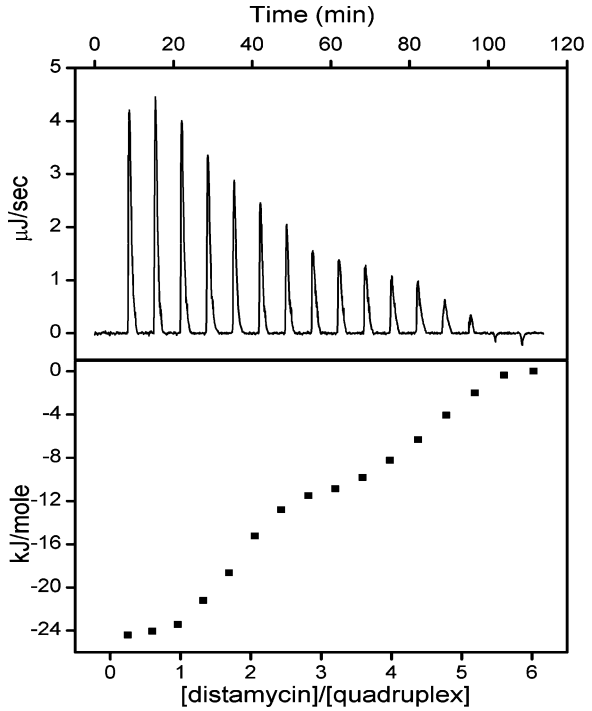

Figure 5. ITC data for the binding of Dist-A to $[d(TGGGGT)]_4$. Top panel shows the calorimetric response of 16 × 15 μL injections of 940 μM Dist-A to 30 μM $[d(TGGGGT)]_4$ at pH 7.3 and $T = 25$ °C. Bottom panel shows the integrated injections heats for the above data.

Table 5. Thermodynamic Parameters for the Interaction of Dist-A with $[d(TGGGGT)]_4$ Determined by ITC at 25 °C

n	K_b ($10^6 \times M^{-1}$)	$\Delta H°$ (kJ mol^{-1})	$T\Delta S°$ (kJ mol^{-1})	$\Delta G°$ (kJ mol^{-1})
1.8 ± 0.2	0.4 ± 0.3	−8 ± 1	24 ± 2	−32 ± 2
4.2 ± 0.2	4.0 ± 3.0	−10 ± 1	27 ± 2	−37 ± 2

Experimental Section). BMI is a numerical parameter that takes into account the relative STD intensities at different saturation frequencies, giving information on the binding contact of the ligand on the target molecule surface.

As for ethidium bromide, the expected BMI value would be ca. 1, as found in the original DF-STD paper,[11] because this small ligand is a base-pairs intercalator[28,29] that establishes secondary electrostatic interactions by extending its two positively charged amino groups toward the phosphate backbone. In analogy to that observed for duplex DNA, the calculated BMI index for ethidium bromide suggests an intercalating binding mode (Table 1). The BMI′ and BMI″ values are consistent with the first one (BMI), confirming the well-defined intercalated position of ethidium bromide.

The above-described experimental data show that the DF-STD approach may be used for describing the intercalating mode of binding of ethidium bromide inside the quadruplex, suggesting that similar information could be derived for characterizing the general binding mode of the Dist-A/quadruplex complex.

The experimental outcomes for Dist-A reveal that the ligand establishes simultaneous interactions with external backbone and aromatic protons of the bases (that face into the groove) (BMI = 0.8), because the saturation diffusion is similar either irradiating on aliphatic protons and on aromatic resonances. Moreover, the BMI value is in agreement with the same one

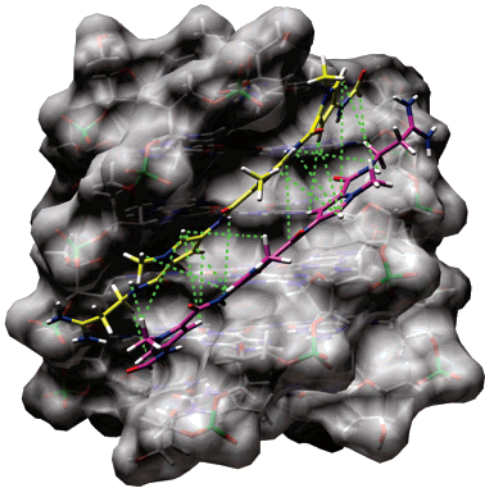

Figure 6. Side view representation of the 4:1 complex Dist-A/$[d(TGGGGT)]_4$. Intermolecular head to tail drug−drug NOE contacts are indicated with green dashed lines.

that describes the well-known interaction of Dist-A with a DNA duplex[11] as minor groove binder. On the other hand, the very low values of both BMI′ and BMI″ (Table 1) show that saturation spreads less than the STD effects obtained irradiating deoxyribose/backbone or purine/pyrimidine bases protons, indicating that Dist-A is closer to the backbone and to the base protons with respect to the imino ones, since these point inside the quadruplex core.

Finally, the whole set of NMR data, along with the structure calculations, confirmed definitively the binding mode of Dist-A with the quadruplex $[d(TGGGGT)]_4$, at least in the experimental condition used here. In particular, the presence of eighteen head to tail drug/drug contacts unambiguously indicates that the drug molecules bind to the quadruplex, two by two, with each term of the dimeric pairs with an antiparallel orientation and in close contact to its partner (as observed with duplex DNA)[6,7] (Figure 6).

Moreover, it is noteworthy that, throughout the whole NMR titration, a single set of signals was present for Dist-A protons, which only grew in intensity and did not show any significant change in chemical shift values by increasing drug concentration. This observation suggests that (i) even at low ligand/DNA stoichiometries (e.g., 0.5:1), simultaneous binding of two Dist-A molecules side by side, in a highly cooperative mode, is dominant; (ii) both in the 2:1 and in the 4:1 complexes, the bound pair of Dist-A molecules, reorientates itself in a fast process on the NMR time scale, similar to that observed for the binding of Dist-A to duplex DNA structures.[6] NOESY spectra acquired at different stages of the titration (data not shown), display the presence of the same head to tail drug/drug contacts observed for the 4:1 complex, and this further supports the above observations.

Furthermore, Dist-A binds two opposite grooves of the quadruplex as suggested also by the presence of NOE contacts only with the H8/H6 protons of strand A and H1′ of strand B (Figure 7).

This explains the dyad symmetry of the final 4:1 complex; that is, it is consistent with a structure comprising two Dist-A dimers simultaneously spanning, in fast reorientation, two opposite grooves of the quadruplex.

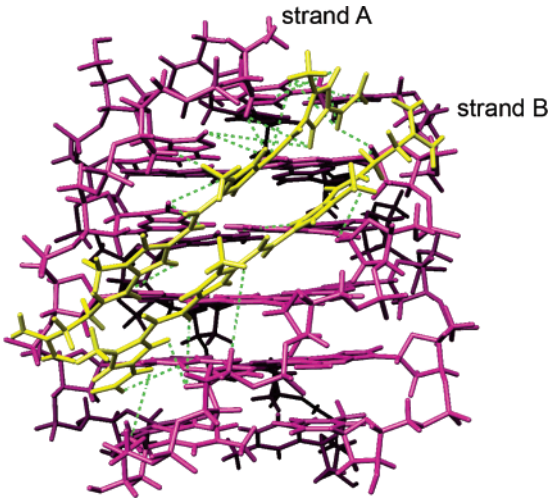

Figure 7. Side view representation of the of the 4:1 complex Dist-A/[d(TGGGGT)]$_4$. Dist-A and [d(TGGGGT)]$_4$ are reported in yellow and magenta, respectively. Drug−DNA NOE contacts are indicated with green dashed lines.

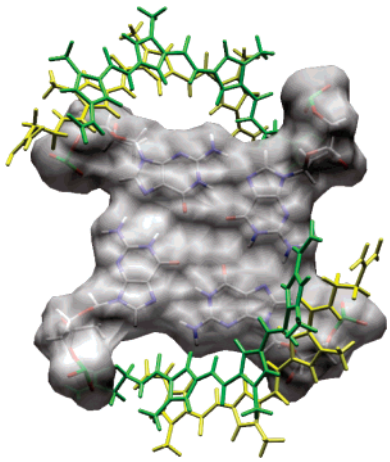

Figure 8. Top view representation of the G3-tetrad showing the different size of the occupied and unoccupied grooves. Dist-A molecules are reported in yellow and green.

To evaluate the changes of the DNA conformation upon binding of Dist-A, we have analyzed by CURVES[35,36] the helix parameters of the most representative structure of the complex (we used lowest energy structure after minimization) and the already reported NMR structure of [d(TTGGGGT)]$_4$ (PDB code: 139D) (see Supporting Information). The DNA quadruplex remains in the B-DNA family, although local variations are observed. The deoxyribose rings are predominantly in a S-type conformation, except for residues G2_Bs which possess a N-type conformation.

Furthermore, as suggested by lower twist values and higher rise values, the helical winding of the complexed DNA is smaller than that of [d(TTGGGGT)]$_4$. Notably, each Dist-A dimer expands its binding groove (similarly to that observed with duplex DNA),[6,7] with concomitant reduction of the size of the adjacent ones. In particular, the bounded grooves are 17.8 Å (∼2 Å wider than that of the uncomplexed quadruplex), while the adjacent ones are 15.0 Å (∼1 Å narrower) (Figure 8). This, basically, prevents a further interaction with other Dist-A molecules.

(35) Lavery, R.; Sklenar, H. *J. Biomol. Struct. Dyn.* **1988**, *6*, 63−91.
(36) Lavery, R.; Sklenar, H. *J. Biomol. Struct. Dyn.* **1989**, *6*, 655−667.

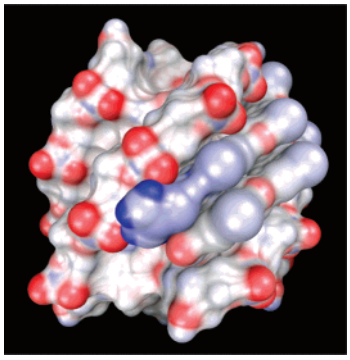

Figure 9. Electrostatic potential surface of the representative structure. The surface is colored according to electrostatic potential, positive potential is shown in blue and negative potential is in red. Electrostatic interactions between amidinium groups of distamycin and G5_A and G4_A phosphate groups of the quadruplex are clearly discernable.

The Dist-A dimers span almost the entire length of the grooves. However, the Dist-A dimers are slightly shifted toward the 5′ end of the quadruplex. The peptide bonds and the *N*-methylpyrrole rings of Dist-A turned out to be planar, while the Dist-A molecules are twisted because of the flexibility of the links between these two planar units. The peptide−pyrrole hinges have similar twist angles of pyrrole−peptide hinges, ranging between 2° and 26°.

The two staggered antiparallel Dist-A molecules overlap by nearly 90%, with each *N*-methylpyrrole ring of one molecule facing a peptide bond of the other one, thus making synchronized twisting to fit the curvature of the DNA quadruplex grooves easier. The preference for such orientation could lie in the electronic $\pi-\pi$ interactions and in the energetically favorable dipole−dipole interactions, since the dipole moments of the pyrrole ring and the carbonyl group are exactly in opposite directions.

The CPK model (see Supporting Information) of the refined structures clearly shows the van der Waals complementarity between Dist-A dimers and the quadruplex grooves. In fact, the crescent shape of the ligand maximizes favorable interactions with the quadruplex by following the curvature of the grooves. Moreover, the negative value for van der Waals energy obtained for the calculated structures (see Table 4) indicates the absence of any unfavorable contacts in the proposed structures.

Electrostatic potential surface has been calculated and visualized with the programs Python,[23] APBS[24] and MSMS.[25] Figure 9 clearly indicates that the positively charged amidinium moiety interacts with the G5_A and G4_A phosphate groups of the quadruplex. Furthermore, the complex is also stabilized by four drug/DNA H-bonds: NH_2-2/G5_A:O2P, NH_2-1/G5_A:N2 and HF/G2_B:N3. It is interesting to note that, when Dist-A binds the duplex DNA,[7] four peptide NH groups of the drug make four hydrogen bonds with N3 (purine) or O2 (pyrimidine) base atoms of DNA. In our case no H-bond involving NH groups has been observed, and this can be explained taking into account that the quadruplex and duplex grooves are chemically different.

Finally, ITC measurements show that the affinity of Dist-A toward [d(TGGGGT)]$_4$ follows the same behavior observed by NMR; there are two distinct binding events, with 2:1 and 4:1 drug/quadruplex stoichiometry, respectively. The affinity between Dist-A and [d(TGGGGT)]$_4$ is enhanced when the ratio of Dist-A to the quadruplex is increased, as the equilibrium constant for the second interaction event is ∼10-fold greater

than that for the first event. It is interesting to note that interaction between Dist-A and the quadruplex is entropically driven, being that the $-T\Delta S°$ value is higher than $\Delta H°$ value. These data confirm once again the groove binding of Dist-A. In fact, a recent analysis made on a number of DNA binding agents revealed that groove-binding is entropically driven, while intercalation is enthalpically driven.[37]

As shortly mentioned in the introduction, Dist-A binds in very different way the quadruplexes $[d(TGGGGT)]_4$[8] and $[d(TAGGGTTA)]_4$ (and its analogues).[9] As demonstrated in this paper, Dist-A binds as dimers in two of the four grooves of the quadruplex $[d(TGGGGT)]_4$, whereas, in the case of $[d(TAGGGTTA)]_4$, two molecules of distamycin A extend over each of the two G-tetrad planes in a 4:1 binding mode. Interestingly, as suggested by the NMR titration profiles, Dist-A seems to possess a higher affinity toward $[d(TGGGGT)]_4$ than $[d(TAGGGTTA)]_4$. In fact, throughout the titration of $[d(TAGGGTTA)]_4$, the signals only underwent a general change in chemical shift resonances and no appearance of a new set of DNA signals was observed. Apparently, there is no specific reason to justify this very different binding mode of Dist-A. Nevertheless, it is known[38] that when a parallel quadruplex structure contains a TA step at the 5′ edge of the sequence, that portion of the complex is less structured. Interestingly, in the structure reported here, Dist-A dimers indeed are not perfectly centered into the quadruplex grooves, but they are slightly shifted toward the 5′-edge. This could mean that Dist-A preferentially recognizes that part of the quadruplex and that, in the case of $[d(TAGGGTT)]_4$ (and its analogues), it is not able to recognize the 5′-end that is unstructured. An alternative explanation could be that the interaction of Dist-A with the grooves of the quadruplex $[d(TAGGGTT)]_4$ could be prevented by motion of the unstructured TA moiety.

In summary, we have proved for the first time that the grooves of a quadruplex structure can be recognized by a small organic molecule. In fact we have demonstrated that distamycin A is able to bind the grooves of the quadruplex $[d(TGGGGT)]_4$. So far, groove binding has been a useful way to selectively recognize only duplex DNA. The results reported here may stimulate the design of new quadruplex groove binders hopefully capable of discriminating between duplex and quadruplex DNA grooves. Then, since groove dimensions vary according to the type of quadruplex,[39] groove binding could also offer the opportunity for obtaining increased selectivity for a particular quadruplex structure.

Acknowledgment. This work is supported by Italian M.U.R.S.T. (P.R.I.N. 2005 and 2006) and Regione Campania (L.41, L.5). The authors are grateful to "Centro di Servizio Interdipartimentale di Analisi Strumentale", C.S.I.A.S., for supplying NMR facilities. The authors are also grateful to Maria Giovanna Chini for supporting us with the preparation of figures.

Supporting Information Available: NOESY data and proton assignments; CPK model; irradiation results. This material is available free of charge via the Internet at http://pubs.acs.org.

JA075710K

(37) Chaires, J. B. *Arch. Biochem. Biophys.* **2006**, *453*, 26−31.
(38) Patel, P. K.; Koti, A. S. R.; Hosur, R. V. *Nucleic Acids Res.* **1999**, *27*, 3836−3843.
(39) Parkinson, G. N. In *Quadruplex Nucleic Acids*; Neidle, S., Balasubramanian, S., Eds.; RSC Publishing: London, 2006; Chapter 1, pp 1−30.